

Article

PVDF membrane morphology - influence of polymer molecular weight and preparation temperature.

Monika Haponska ¹, Anna Trojanowska ^{2,*}, Adrianna Nogalska³, Renata Jastrzab ⁴, Tania Gumi ⁵ and Bartosz Tylkowski ^{6,*}

¹ Departament d'enginyeria química, Universitat Rovira i Virgili, Av. dels Països Catalans 26, 43007 Tarragona, Spain; A. Mickiewicz University, Faculty of Chemistry, Umultowska 89b, 61-614 Poznan, Poland monika.haponska@urv.cat

² Departament d'enginyeria química, Universitat Rovira i Virgili, Av. dels Països Catalans 26, 43007 Tarragona, Spain; A. Mickiewicz University, Faculty of Chemistry, Umultowska 89b, 61-614 Poznan, Poland; anna.trojanowska@urv.cat

³ Departament d'enginyeria química, Universitat Rovira i Virgili, Av. dels Països Catalans 26, 43007 Tarragona, Spain; A. Mickiewicz University, Faculty of Chemistry, Umultowska 89b, 61-614 Poznan, Poland; adrianna.nogalska@urv.cat

⁴ A. Mickiewicz University, Faculty of Chemistry, Umultowska 89b, 61-614 Poznan, Poland; renatad@amu.edu.pl

⁵ Departament d'enginyeria química, Universitat Rovira i Virgili, Av. dels Països Catalans 26, 43007 Tarragona, Spain; tania.gumi@urv.cat

⁶ Centre Tecnològic de la Química de Catalunya, Carrer de Marcel·lí Domingo, 43007 Tarragona, Spain

* Correspondence: bartosz.tylkowski@ctqc.org; Tel.: +34-977-297-086

Abstract: The global polyvinylidene fluoride market is estimated to reach \$937,278.5 thousand by 2019, therefore to develop new membranes and gain pioneering ideas, which could create innovative business opportunities, a fundamental knowledge about membrane properties fabricated from recent commercially available PVDF polymers is highly mandatory. In this study, we successfully prepared nine non-woven supported PVDF membranes using a phase inversion precipitation method starting from a 15 wt% PVDF solution in N-methyl-2-pyrrolidone. Various membrane morphologies were obtained by using (1) PVDF polymers with diverse molecular weight in a range from 300.000 Da to 700.000 Da and (2) different temperatures of the coagulation bath (20, 40, and 60 \pm 2°C) used for the films precipitation. Environmental Scanning Electron Microscope (ESEM) was used for surface and cross-section morphologies characterization. Atomic Force Microscope (AFM) was employed to investigate surface roughness, while Contact Angle (CA) instrument was used for membranes wettability studies. Fourier Transform Infrared Spectroscopy (FTIR) results show that the fabricated membranes are formed by a mixture of TGTG' chains in α phase crystalline domains and all-TTTT trans planar zigzag chains characteristic to β phase. Moreover, generated results indicate that the phases content and membrane morphologies depend on the polymer molecular weight and conditions used for the membranes preparation. The diversity of fabricated membranes could be applied by the End User Industries for different applications.

Keywords: PVDF membrane; coagulation bath temperature; polymer molecular weight

1. Introduction

Polyvinylidene fluoride (PVDF) is one of the most widely studied and well accepted polymer for membrane fabrication through conventional phase inversion method considering its unique features including: good degradation resistance against radiation, excellent chemical and thermal resistance as well as excellent mechanical properties [1-3]. It is a specialty plastic used in vast number of traditional, well-defined applications such as: piping & tubing, membrane, cable and an insulator for premium wire wherein the high purity, and emerging ones, such as: lithium-ion batteries, coatings for new energy and electronics devices, photovoltaic films, or medical applications [4-7]. To meet booming global demand for this thermoplastic polymer in energy-efficient, environmental and industrial applications, very recently (November, 2017) Solvay S.A. Company – one of the industrial leaders in PVDF production - inaugurated its Solef® polyvinylidene fluoride (PVDF) plant in China [8]. According to a report: “Polyvinylidene Fluoride (PVDF) Market: Global Industry Analysis and Opportunity Assessment 2014 – 2020” recently published, another important PVDF manufacturers dominating the market are the following companies: Arkema, Daikin Industries Ltd., Dyneon GmbH, Shanghai Ofluorine Chemical Technology Co. Ltd., Shanghai 3F New Materials Company Limited, Zhuzhou Hongda Polymer Materials Co. Ltd., Zhejiang Fotech International Co. Ltd., Kureha Corporation, Quadrant Engineering Plastics Products Inc.; however, the Research & Development has been one of the key factors in the PVDF final products design [9]. Depending on the polymerization process (emulsion polymerization, suspension polymerization, etc.), PVDF with different molecular weight distributions are available, which is a critical factor for the final performance of the prepared membranes [10]. It is well known that the molecular weight of the polymer has a significant effect on the rheology of the polymer solution and on the thermodynamic and kinetic aspects of the phase inversion, which influences the structure and performance of the final membranes [11]. Knowledge of polymer crystallinities and their resulting membrane morphologies is important as a basis of understanding its membrane permeability and selectivity, as well as its various chemical and mechanical properties [12]. Researchers have investigated the influence of an addition of a small concentration of various components on membrane structure. These additives often show specific interactions with one of the other three components. Indeed, a number of publications focused on composited PVDF membranes has been published during the last decade [4,13-16]. However, new methods and strategies have been applied for the PVDF polymers production, which could impact their polymorphs [17-19]. Thus, to design new membranes and gain innovative ideas, which could lead to new break-through business opportunities, a fundamental knowledge about membrane properties obtained from current commercially available PVDF polymers is highly required. For this reason, our research has been focused on PVDF membrane preparation applying the phase inversion precipitation method with coagulation bath at different temperature in a range 20-60 °C. In addition, influence of different PVDF molecular weight on membrane morphology has been investigated.

2. Materials and Methods

2.1. Materials

PVDF powders: Solef 6010, Solef 1015 and Solef 6020, were kindly donated by Solvay Specialty Polymers (Bollate, Italy). N-methyl-2-pyrrolidone (NMP, 99%) was provided by Panreac (Spain). Non-woven Hollytex 34 GR was provided by STEM Company. Distilled water was used as non-solvent in coagulation bath.

2.2. Preparation of PVDF membranes

PVDF membranes were prepared by the immersion precipitation method. In brief, PVDF pellets were dissolved in NMP at 80°C with vigorous stirring for 48 h to form a homogeneous casting solution. After air bubbles were removed completely, the resulting solution was cooled to the room temperature $20 \pm 2^\circ\text{C}$, spread uniformly onto a glass plate with non-woven attached using a casting

knife with a 250- μm gate opening (K Paint Applicator, R K Print Coat Instruments, Ltd., U.K.), and then immersed immediately into a precipitation bath of deionized water set up at different temperatures: 20 \pm 2°C, 40 \pm 2°C, or 60 \pm 2°C. The formed solid membranes were washed thoroughly with deionized water to remove residual solvent and dried at about 40°C for 24 h under vacuum before further characterization.

2.3. Membrane characterization

The crystalline forms of the PVDF membranes were investigated by Fourier Transform Infrared Spectroscopy VERTEX 70, equipped with a Platinum-ATR-accessory with 2 cm^{-1} resolution and 32 scans.

The cross sections and the surface morphologies of the fabricated PVDF membranes were characterized by Environmental Scanning Electron Microscopy (Quanta 600, FEI) [20]. Cross sections were prepared by fracturing in liquid nitrogen the membranes that were previously wet in ethanol. The pore size was calculated by means of IFME software and the ESEM micrographs of the membrane cross sections.

Agilent 5500 Environmental Atomic Force Microscope (AFM, Agilent Technology) equipped with an extender electronics module was used to investigate membrane surface morphologies. The AFM micrographs (2 \times 2 μm) were captured at room temperature in tapping mode using Multi 75 (BudgetSensors) silicon cantilevers (length = 225 μm , width = 28 μm , and thickness = 3 μm) with a force constant of 3 N/m, 75 kHz resonance frequency and 0.7–2 Hz scan rate. During the AFM experiments, the studied samples were located on an active vibration isolation chamber (Agilent Technology), which protect them from external vibration and eliminate external noise. Generated images were analyzed by The Nanotec WSxM 5.0 Develop 4.0 software.

Contact angles of water drops on a membrane surface were measured with Dataphysics OCA 15EC apparatus. The 3 μm drops of water, dripped from a microsyringe, were placed on the membrane at room temperature. The contact angle was measured immediately after putting the water drop on the membrane surface. Measurements were repeated using different areas of the material: for each test reported, at least five drops of water were used.

3. Results and Discussion

It is well known that the PVDF crystals have three different molecular conformations: trans-gauche-trans-gauche' (TGTG'), trans-trans-trans (TTT), trans-trans-trans-gauche (TTTG), and five different polymorphs: α (phase II), β (phase I), γ (phase III), δ , and ϵ [15,21]. Each of the polymorphs possess its unique properties which could affect the morphology and performance of the fabricated membrane. It has been found that β -phase PVDF has some specific properties such as polarity and higher mechanical strength compared with α -phase [4]. As it is shown in Table 1, we prepared 9 membranes, named M1-M9, applying the phase inversion precipitation method with NMP as a solvent and distilled water as a nonsolvent at different temperatures of coagulation baths. Membranes M1, M4, M7 were precipitated at 20 \pm 2°C, while membranes M2, M5, M8, and membranes M3, M6, M9 were obtained at 40 \pm 2°C and 60 \pm 2°C, respectively. Furthermore, membranes M1-M3 were done using PVDF with 300.000-320.000 Da molecular weight, while membranes M4-M6 and M7-M9 were fabricated using PVDF with 570.000-600.000 Da and 670.000-700.000 Da, respectively. To verify influences of (i) coagulation bath temperature and (ii) molecular weights of PVDF on the polymorphism of the investigated membranes, infra-red spectroscopy, which is a common method for the PVDF crystalline phase characterization [21], was carried out.

Table 1. M1-M9 membranes preparation parameters and characteristics of the resulting membranes.

Membrane	Molecular weight of polymer [Da]	Temperature of coagulation bath [°C]	β/α phase ratio	Main pore size [μm]	RMS roughness	Contact angle [°]	Thickness of membrane [μm]
M1	300,000 – 320,000	20 \pm 3	0.71	0.42 \pm 0.01	16.07 \pm 0.08	68.7 \pm 3.4	106 \pm 2
M2		40 \pm 3	0.29	0.37 \pm 0.02	12.08 \pm 0.07	61.2 \pm 1.0	103 \pm 2
M3		60 \pm 3	0.17	0.18 \pm 0.03	17.18 \pm 0.11	78.0 \pm 5.4	106 \pm 2
M4	570,000 – 600,000	20 \pm 3	0.59	0.38 \pm 0.04	15.17 \pm 0.15	74.5 \pm 9.0	107 \pm 2
M5		40 \pm 3	0.26	0.22 \pm 0.03	11.26 \pm 0.13	59.0 \pm 2.8	120 \pm 2
M6		60 \pm 3	0.12	0.16 \pm 0.02	16.56 \pm 0.17	79.9 \pm 4.9	113 \pm 2
M7	670,000 – 700,000	20 \pm 3	0.53	0.27 \pm 0.02	15.71 \pm 0.29	68.3 \pm 3.8	114 \pm 2
M8		40 \pm 3	0.24	0.20 \pm 0.03	12.15 \pm 0.14	65.2 \pm 6.6	106 \pm 2
M9		60 \pm 3	0.11	0.15 \pm 0.02	18.27 \pm 0.23	98.1 \pm 5.9	115 \pm 2

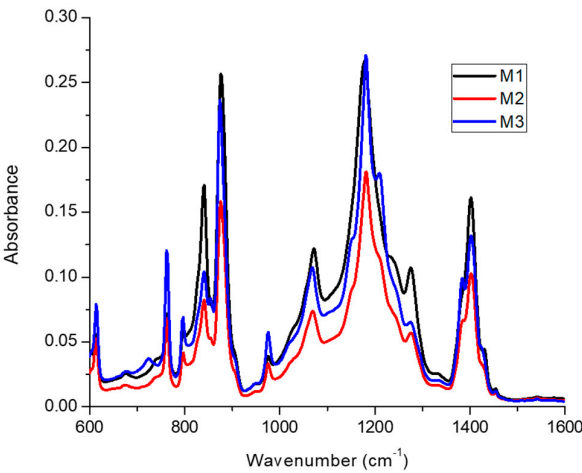


Figure 1. FTIR-ATR spectra of showing characteristics peaks for α and β phases of membranes M1, M2 and M3 prepared from the same molecular weight of PVDF at different temperature.

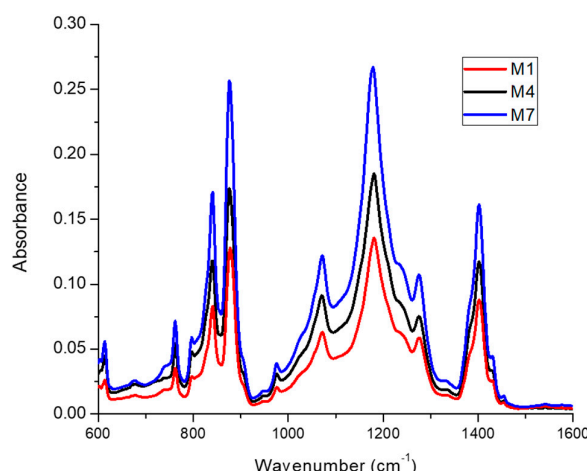


Figure 2. FTIR-ATR spectra of showing characteristics peaks for α and β phases of membranes M1, M4 and M7 prepared at the same temperature using PVDF with different molecular weights.

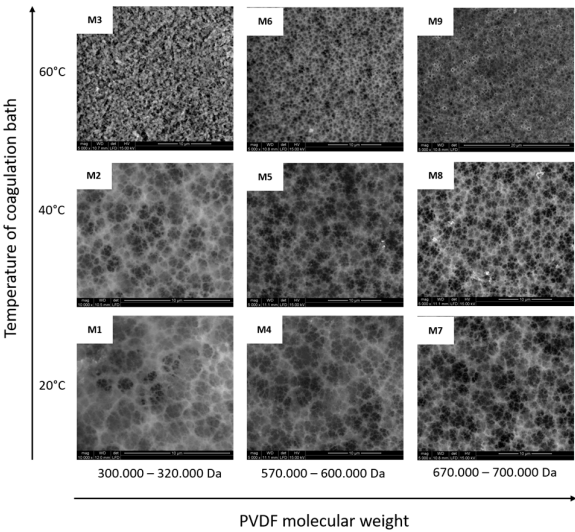
Figure 1 shows the FTIR-ATR spectra of M1, M2 and M3 membranes, fabricated from 15 wt% PVDF 300.000 – 320.000 Da polymeric solution at 20, 40, and 60 °C, respectively, while Figure 2 shows the spectra of M1, M4, M7 precipitated at 20 °C from 15wt% PVDF solutions with molecular weights of 300.000 – 320.000 Da, 570.000 – 600.000 Da, and 670,000 – 700,000 Da, respectively. As it has been reported in literature [22,23], the presence of representative bands at 612, 762, 796, 855, 975, and 1400 cm^{-1} indicates the formation of α phase while the vibration bands at 840 and 1234 cm^{-1} suggest the existence of the orthorhombic β phase. Furthermore, the absence of bands at 833 and 1233 cm^{-1} excludes the γ phase. Beside due to the consistency of C–F stretch at 1182 cm^{-1} the PVDF membranes have good stability to the thermal and chemical treatments [16]. The FTIR-ATR results suggest that the investigated membranes are formed by a mixture of TGTG' chains in α phase crystalline domains and all-TTTT trans planar zigzag chains characteristic to β phase. To estimate α or β phase ascendancy in the membrane structure β/α phase ratios were calculated for all M1-M9 membranes and they are given in Table 1. These values were calculated by comparing the absorbencies of vibration band peaks at 840 cm^{-1} (CH_2 rocking) and 762 cm^{-1} (CF_2 bending and skeletal bending) using the following equation [24]:

$$\frac{F(\beta)}{F(\alpha)} = \frac{A_{\beta}^{840}}{(K_{\beta}^{840}d^{840}/K_{\alpha}^{762}d^{762})A_{\alpha}^{762}} = \frac{A_{\beta}^{840}}{1.15A_{\alpha}^{762}} \quad (1)$$

where $F(\beta)$ and $F(\alpha)$ are mass fractions of β and α phase; A_{β}^{840} and A_{α}^{762} are the baseline-corrected absorption peaks of the β and α phases at 762 and 840 cm^{-1} , respectively. K and d are the absorption coefficient and penetration depth at the corresponding wavenumber, respectively. $K_{\beta}^{840} = 7.7 \cdot 104 \text{ cm}^2/\text{mol}$; $K_{\alpha}^{762} = 6.1 \cdot 104 \text{ cm}^2/\text{mol}$; $d^{840} = 0.79 \mu\text{m}$; $d^{762} = 0.87 \mu\text{m}$ were used based on literature findings [24].

Generated results clearly demonstrate that the membrane polymorphism strongly depends on temperature of non-solvent used for its precipitation. The β phase mostly dominates in the membrane fabricated at 20 °C; while the α phase content increases with the coagulation bath temperature increases (up to 60 °C). According to Wang et al. [25] during the immersion of the casting solutions to the non-solvent at lower temperature (15 °C) a delayed liquid–liquid demixing mechanism occurs. This mechanism could encourage a gelation process indicated by formation of microcrystallites and the β phase. On the other hand, the temperature increase favors the mobility of PVDF chains which

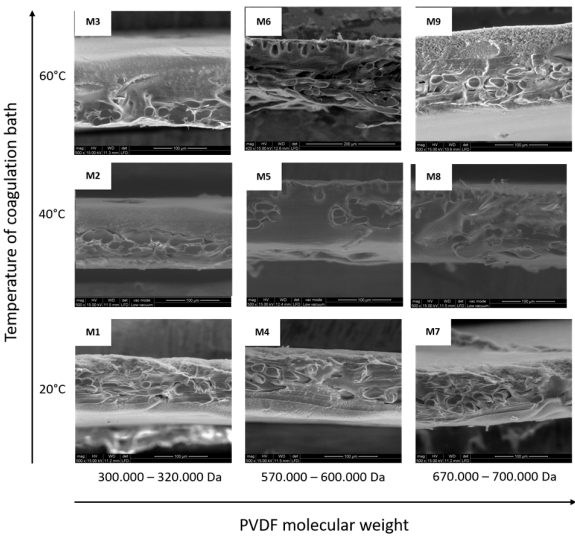
178 facilitates the formation of stable non-polar α phase with a monolithic lattice structure. These
179 observations are consistent with literature findings: Gradys and Sajkiewicz [26] stated that the
180 thermodynamically less stable β phase is typically formed at room temperature, while Gregorio [27]
181 reported that the α phase normally forms at high temperature. Moreover, comparing the values of
182 β/α phase ration given in Table 1, for the membranes formed at the same temperature but from
183 different molecular weight PVDF solutions (i.e. M1-M4-M7; M2-M5-M8; M3-M6-M9) the increase of
184 β phases can be observed with the molecular weight increase. We think that it could take place due
185 to significant polymer chain entanglements at higher molecular weights, which lead to the oriented
186 packing of $\text{CH}_2\text{-CF}_2$ dipoles, thus supporting the formation of β phase crystals.
187



188

189 Figure 3. ESEM micrographs of M1-M9 membrane top surfaces.

190



191

192 Figure 4. ESEM micrographs of M1-M9 membrane cross-sections.

Figure 3 shows the ESEM micrographs of M1-M9 membrane top surfaces, while Figure 4 provides their cross-sections. Membrane thicknesses, calculated by Image-ProPlus 5 software on ESEM cross-section micrographs [28], are in a range of $103\text{--}120 \pm 2 \mu\text{m}$ (see Table 1). According to literature [29] membrane thickness usually decreases with the increase of polymer viscosity (modulated by polymer molecular weight); however, in our studies this trend has not been registered, probably due to the presence of non-woven support which structure is well filled by the polymers and forms an integrated part of the membranes. As it can be observed in Figures 3 membranes M1, M4, M7 prepared at 20°C possess three dimensional fibriform network morphologies. In our opinion it is caused due to the PVDF semicrystallinity. Indeed, Wang et al. [25] observed that at low temperature the β phase microcrystallites connect various polymeric chains together, and form these 3D fibriform networks similar to those demonstrated in Figure 3. Moreover, the ESEM investigation shows that the PVDF membrane surface morphology is strongly influenced by temperature of coagulation bath. Thus, surface porosity was verified by providing pore mean size distributions, which were calculated using IFME software basing on the ESEM surface micrographs [30]. As it is given in Table 1, the pore main size of measured at M1-M9 membrane top surfaces is in a range $0.18\text{--}0.49 \pm 0.26 \mu\text{m}$ and its value is related to the temperature of the non-solvent in which the membrane was precipitated and to the molecular weight of the polymer used for membrane fabrication. Comparing the values given in Table 1 we can conclude that with temperature and molecular weight increase the pore main size decreases what is in accordance with literature data. Cardoso et al. [31] stated that increasing water bath temperature leads to less porous membrane surfaces. The effect of PVDF molecular weight on surface porosity was studied by Hassankiadeh and co-authors [32] who have investigated PVDF hollow fiber membranes using PVDF Solef 1015 and 6020, with molecular weight rates $570.000\text{--}600.000$ and $670.000\text{--}700.000$, respectively. The authors reported that the pore main size of the fiber surfaces decreases with the PVDF molecular weights increase. Matsuyama and co-authors [33] reported that reducing the viscosity of the polymer solution by decreasing the polymer molecular weight helps the solvent displacement which provides the possibility of improved symmetry of the membrane structure in the lower molecular weight polymer compared with that in the higher molecular weight polymer, what has a significant impact on membrane porosity and pore main size. Further inspection of the ESEM images reveals that the membrane cross-sections morphologies (Figure 4) are strongly affected by the polymer molecular weight. As it can be observed in the micrographs, membranes M2 and M3 possess compacted structure, while membrane M4 and M5 possess drop-like macrovoids at the top part and dense sponge-like structures at the bottom part. Membranes M7 and M8 possess mostly spongy-like structures. From the kinetic point of view, the increase in viscosity with an increase in the PVDF molecular weight decreases the solvent/nonsolvent exchange rate by increasing kinetic hindrance in the phase inversion process. Thus, the delayed demixing is endorsed, resulting in the formation of less drop-like structure and more sponge-like structure. Therefore, the drop-like structure are predictable to be formed in the intermediate range of molecular weight as a result of the superimposition of the thermodynamic and the kinetic effect, if the thermodynamic effect controls the phase inversion process earlier than the kinetic effect [34].

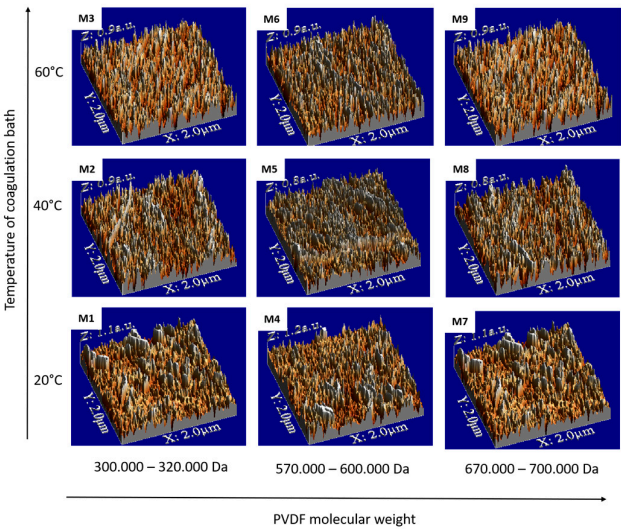


Figure 5. AFM images of M1-M9 membrane top surfaces.

The surface roughness of the membranes has important consequence on transport phenomena and has been the topic of numerous investigations [2,32,35]. Figure 5 shows the AFM images of the top surface of the M1-M9 PVDF membranes, while the root mean square (RMS) roughness, considered as a standard deviation of height, is listed in Table 1. Comparing the RMS values, it can be seen that the smoother membranes were obtained at 40 °C. These results are of actual attention for technological applications where smooth, uniform, homogeneous, and porous membranes are needed, such as scaffolds for cells growth or separator of lithium ion batteries [36]. It is commonly known that the roughness parameter is linked to the contact angle of the membrane and its wettability [37]. At it has been reported in literature [30,37,38] surface roughening tends to increase the contact angle values. Table 1 provides the static contact angle results measured on M1–M9 membranes. The contact angle results show that the highest value $98.1 \pm 5.9^\circ$ was measured for the membrane M9 with the highest RMS value, and the lowest value $59.0 \pm 2.8^\circ$ was measured for the smoother M5 membrane. This diversity of membrane surface wettability as well as cross-section and surface morphologies could find broad application fields, such as medicine, water purification, separation and concentration of biologically active compounds, etc. depending on the End User Industries individual profiles and requirements.

4. Conclusions

By using phase inversion precipitation techniques nine PVDF based membranes were fabricated at 20, 40 and 60 °C using three different polymer molecular weight: 300.000-320.000 Da, 570.00-600.000 Da and 670.000-700.000 Da. Based on FTIR-ATR investigation it was observed that membrane polymorphism is influenced on polymer molecular weight and temperature of non-solvent used for membrane precipitation. The membrane with dominated β phase are formed at lower temperature and using the PVDF with the highest molecular weight. Furthermore, by ESEM investigation with IFME software it was observed that the presence of the β phase has a significant impact on membrane morphology and favors three dimensional fibriform network surface structure formation. Moreover, achieved results demonstrated that cross-section membrane morphologies are impacted by PVDF molecular weight: at low molecular weight compact membrane were produced, while at intermediate and at high molecular weights weight drop-like and spongy-like membranes were fabricated, respectively. AFM and Contact angle studies show that the smoother membranes were produced at 40 °C using intermediate polymer molecular weight.

Acknowledgments:

The authors would like to thank European Commission for the Erasmus fellowship, under which the students from the Adam Mickiewicz University, Poznan, Poland have been able to visit Univeristat Rovira Virgili, Tarragona, Spain and participate in this research project. Furthermore, we would like to thanks Solvay S.A for donation the PVDF polymers.

Author Contributions:

Dr. Bartosz Tylkowski and Ms. Monika Haponska conceived and designed the experiments; Ms. Haponska fabricated the membranes; Ms. Anna Trojanowska and Ms. Adrianna Nogalska performed the AFM and CA analysis. Dr. Tania Gumi and Prof. Renata Jastrzab carried out FTIR-ATR and ESEM investigations. Dr. Tylkowski and Ms. Trojanowska wrote the paper.

Conflicts of Interest: "The authors declare no conflict of interest."

References

1. Younas, H.; Bai, H.; Shao, J.; Han, Q.; Ling, Y.; He, Y. Super-hydrophilic and fouling resistant pvdf ultrafiltration membranes based on a facile prefabricated surface. *Journal of Membrane Science* **2017**, *541*, 529-540.
2. Li, N.; Fu, Y.; Lu, Q.; Xiao, C. Microstructure and performance of a porous polymer membrane with a copper nano-layer using vapor-induced phase separation combined with magnetron sputtering. *Polymers* **2017**, *9*, 524.
3. Chen, F.; Shi, X.; Chen, X.; Chen, W. Preparation and characterization of amphiphilic copolymer pvdf-g-pmabs and its application in improving hydrophilicity and protein fouling resistance of pvdf membrane. *Applied Surface Science* **2018**, *427*, 787-797.
4. Golzari, N.; Adams, J.; Beuermann, S. Inducing β phase crystallinity in block copolymers of vinylidene fluoride with methyl methacrylate or styrene. *Polymers* **2017**, *9*, 306.
5. Burnham-Fay, E.D.; Le, T.; Tarbuton, J.A.; Ellis, J.D. Strain characteristics of additive manufactured polyvinylidene fluoride (pvdf) actuators. *Sensors and Actuators A: Physical* **2017**, *266*, 85-92.
6. Kwon, J.; Choi, S. Method of manufacturing pvdf-based polymer and method of manufacturing multilayered polymer actuator using the same. Google Patents: 2013.
7. Liu, T.; Chang, Z.; Yin, Y.; Chen, K.; Zhang, Y.; Zhang, X. The pvdf-hfp gel polymer electrolyte for li-o₂ battery. *Solid State Ionics* **2017**.
8. Solvay. https://www.Solvay.Com/en/media/press_releases/20171107-pvdf-polymer-presence-global-new-unit-china.Html.
9. Company, F.M.I. Polyvinylidene fluoride (pvdf) market: Global industry analysis and opportunity assessment 2014 - 2020 <https://www.futuremarketinsights.com/reports/global-polyvinylidene-fluoride-market>
10. Tan, Z.; Wang, X.; Fu, C.; Chen, C.; Ran, X. Effect of electron beam irradiation on structural and thermal properties of gamma poly (vinylidene fluoride) (γ -pvdf) films. *Radiation Physics and Chemistry*.
11. Kang, G.-d.; Cao, Y.-m. Application and modification of poly(vinylidene fluoride) (pvdf) membranes – a review. *Journal of Membrane Science* **2014**, *463*, 145-165.
12. Meng, N.; Mao, R.; Tu, W.; Odolczyk, K.; Zhang, Q.; Bilotti, E.; Reece, M.J. Crystallization kinetics and enhanced dielectric properties of free standing lead-free pvdf based composite films. *Polymer* **2017**, *121*, 88-96.
13. Farooqui, U.R.; Ahmad, A.L.; Hamid, N.A. Effect of polyaniline (pani) on poly(vinylidene fluoride-co-hexafluoro propylene) (pvdf-co-hfp) polymer electrolyte membrane prepared by breath figure method. *Polymer Testing* **2017**, *60*, 124-131.
14. Ike, I.A.; Dumée, L.F.; Groth, A.; Orbell, J.D.; Duke, M. Effects of dope sonication and hydrophilic polymer addition on the properties of low pressure pvdf mixed matrix membranes. *Journal of Membrane Science* **2017**, *540*, 200-211.

- 315 15. Kong, Y.; Ma, Y.; Lei, L.; Wang, X.; Wang, H. Crystallization of poly(ϵ -caprolactone) in
316 poly(vinylidene fluoride)/poly(ϵ -caprolactone) blend. *Polymers* **2017**, *9*, 42.
- 317 16. Davenport, D.; Gui, M.; Ormsbee, L.; Bhattacharyya, D. Development of pvdf membrane
318 nanocomposites via various functionalization approaches for environmental applications.
319 *Polymers* **2016**, *8*, 32.
- 320 17. Bonnet, A.; Mathieu, C.; REYNA-VALENCIA, A.; RAMFEL, B.; DEGOULET, C. Fluorinated
321 polymer composition. Google Patents: 2017.
- 322 18. Kappler, P.; Gauthe, V. Process for the manufacture of thermally stable pvdf. Google Patents:
323 2004.
- 324 19. Pascal, T. Vinylidene fluoride polymer having a fraction of non-transferred chains and its
325 manufacturing process. Google Patents: 2006.
- 326 20. Binczyk, M.; Nowak, M.; Skrobanska, M.; Tylkowski, B.; Runka, T.; Jastrzab, R. Silver cd-r
327 based substrate as a sers active material. *Journal of the Iranian Chemical Society* **2016**, *13*, 841-
328 845.
- 329 21. Cui, Z.; Drioli, E.; Lee, Y.M. Recent progress in fluoropolymers for membranes. *Progress in*
330 *Polymer Science* **2014**, *39*, 164-198.
- 331 22. Cui, Z.; Hassankiadeh, N.T.; Zhuang, Y.; Drioli, E.; Lee, Y.M. Crystalline polymorphism in
332 poly(vinylidene fluoride) membranes. *Progress in Polymer Science* **2015**, *51*, 94-126.
- 333 23. Munirasu, S.; Banat, F.; Durrani, A.A.; Haija, M.A. Intrinsically superhydrophobic pvdf
334 membrane by phase inversion for membrane distillation. *Desalination* **2017**, *417*, 77-86.
- 335 24. Zhang, M.; Zhang, A.-Q.; Zhu, B.-K.; Du, C.-H.; Xu, Y.-Y. Polymorphism in porous
336 poly(vinylidene fluoride) membranes formed via immersion precipitation process. *Journal of*
337 *Membrane Science* **2008**, *319*, 169-175.
- 338 25. Wang, X.; Zhang, L.; Sun, D.; An, Q.; Chen, H. Effect of coagulation bath temperature on
339 formation mechanism of poly(vinylidene fluoride) membrane. *Journal of Applied Polymer*
340 *Science* **2008**, *110*, 1656-1663.
- 341 26. Grady, A.; Sajkiewicz, P. Determination of the melting enthalpy of β phase of
342 poly(vinylidene fluoride) *e-polymers* **2013**, *19*, 1-14.
- 343 27. Gregorio, R. Determination of the α , β , and γ crystalline phases of poly(vinylidene fluoride)
344 films prepared at different conditions. *Journal of Applied Polymer Science* **2006**, *100*, 3272-3279.
- 345 28. Tylkowski, B.; Carosio, F.; Castañeda, J.; Alongi, J.; García-Valls, R.; Malucelli, G.;
346 Giamberini, M. Permeation behavior of polysulfone membranes modified by fully organic
347 layer-by-layer assemblies. *Industrial & Engineering Chemistry Research* **2013**, *52*, 16406-16413.
- 348 29. Chen, Z.; Rana, D.; Matsuura, T.; Meng, D.; Lan, C.Q. Study on structure and vacuum
349 membrane distillation performance of pvdf membranes: II. Influence of molecular weight.
350 *Chemical Engineering Journal* **2015**, *276*, 174-184.
- 351 30. Nogalska, A.; Ammendola, M.; Tylkowski, B.; Ambrogio, V.; Garcia-Valls, R. Ambient co₂
352 adsorption via membrane contactors – value of assimilation from air as nature stomata.
353 *Journal of Membrane Science* **2018**, *546*, 41-49.
- 354 31. Cardoso, V.F.; Botelho, G.; Lanceros-Méndez, S. Nonsolvent induced phase separation
355 preparation of poly(vinylidene fluoride-co-chlorotrifluoroethylene) membranes with
356 tailored morphology, piezoelectric phase content and mechanical properties. *Materials &*
357 *Design* **2015**, *88*, 390-397.
- 358 32. Hassankiadeh, N.T.; Cui, Z.; Kim, J.H.; Shin, D.W.; Sanguineti, A.; Arcella, V.; Lee, Y.M.;
359 Drioli, E. Pvdh hollow fiber membranes prepared from green diluent via thermally induced
360 phase separation: Effect of pvdf molecular weight. *Journal of Membrane Science* **2014**, *471*, 237-
361 246.
- 362 33. Matsuyama, H.; Maki, T.; Teramoto, M.; Asano, K. Effect of polypropylene molecular weight
363 on porous membrane formation by thermally induced phase separation. *Journal of Membrane*
364 *Science* **2002**, *204*, 323-328.
- 365 34. Smolders, C.A.; Reuvers, A.J.; Boom, R.M.; Wienk, I.M. Microstructures in phase-inversion
366 membranes. Part 1. Formation of macrovoids. *Journal of Membrane Science* **1992**, *73*, 259-275.

- 367 35. Zhong, Z.; Li, D.; Zhang, B.; Xing, W. Membrane surface roughness characterization and its
368 influence on ultrafine particle adhesion. *Separation and Purification Technology* **2012**, *90*, 140-
369 146.
- 370 36. Sousa, R.E.; Nunes-Pereira, J.; Costa, C.M.; Silva, M.M.; Lanceros-Méndez, S.; Hassoun, J.;
371 Scrosati, B.; Appetecchi, G.B. Influence of the porosity degree of poly(vinylidene fluoride-co-
372 hexafluoropropylene) separators in the performance of li-ion batteries. *Journal of Power*
373 *Sources* **2014**, *263*, 29-36.
- 374 37. Tylkowski, B.; Tsibranska, I. Overview of main techniques used for membrane
375 characterization. *Journal of Chemical Technology and Metallurgy* **2015**, *50*, 3-12.
- 376 38. Bogdanowicz, K.A.; Tylkowski, B.; Giamberini, M. Preparation and characterization of light-
377 sensitive microcapsules based on a liquid crystalline polyester. *Langmuir* **2013**, *29*, 1601-1608.